High-cholesterol diet in combination with hydroxypropyl-β-cyclodextrin induces NASH-like disorders in the liver of rats

Yasuka Saigo[1,2], Tomohiko Sasase[1,2], Marika Tohma[3], Kinuko Uno[3], Yuichi Shinozaki[1,2], Tatsuya Maekawa[1], Ryuhei Sano[1,3], Katsuhiro Miyajima[3], Takeshi Ohta[2]

1 Biological/Pharmacological Research Laboratories, Takatsuki Research Center, Central Pharmaceutical Research Institute, Japan Tobacco Inc., Takatsuki, Osaka 569-1125, Japan
2 Laboratory of Animal Physiology and Functional Anatomy, Graduate School of Agriculture, Kyoto University., Sakyo-ku, Kyoto 606-8502, Japan
3 Department of Nutritional Science and Food Safety, Faculty of Applied Biosciences, Tokyo University of Agriculture., Setagaya-ku, Tokyo 156-8502, Japan

Corresponding author
Tomohiko Sasase, Ph.D.
Biological/Pharmacological Research Laboratories, Takatsuki Research Center, Central Pharmaceutical Research Institute, Japan Tobacco Inc., Takatsuki, Osaka 569-1125, Japan, E-mail: tomohiko.sasase@jt.com

Short title
A novel rat model of NASH; cholesterol induces pathogenesis

Summary
Non-alcoholic fatty liver disease (NAFLD) is a general term for fatty liver disease not caused by viruses or alcohol. Fibrotic hepatitis, cirrhosis, and hepatocellular carcinoma can develop. The recent increase in NAFLD incidence worldwide has stimulated drug development efforts. However, there is still no approved treatment. This may be due in part to the fact that non-alcoholic steatohepatitis (NASH) pathogenesis is very complex, and its mechanisms are not well understood. Studies with animals are very important for understanding the pathogenesis. Due to the close association between the establishment of human NASH pathology and metabolic syndrome, several animal models have been reported, especially in the context of overnutrition. In this study, we investigated the induction of NASH-like pathology by enhancing cholesterol absorption through treatment with hydroxypropyl-β-cyclodextrin (CDX). Female Sprague-Dawley rats were fed a normal diet with normal water (control group); a high-fat (60 kcal%), cholesterol (1.25%), and cholic acid (0.5%) diet with normal water (HFCC group); or HFCC diet with 2% CDX water (HFCC+CDX group) for 16 weeks. Compared to the control group, the HFCC and HFCC+CDX groups showed increased blood levels of total

cholesterol, aspartate aminotransferase, and alanine aminotransferase. At autopsy, parameters related to hepatic lipid synthesis, oxidative stress, inflammation, and fibrosis were elevated, suggesting the development of NAFLD/NASH. Elevated levels of endoplasmic reticulum stress-related genes were evident in the HFCC+CDX group. In the novel rat model, excessive cholesterol intake and accelerated absorption contributed to NAFLD/NASH pathogenesis.

Key words

NAFLD, NASH, cholesterol, hydroxypropyl-β-cyclodextrin

Introduction

Non-alcoholic fatty liver disease (NAFLD) is a general term for chronic liver disease in which a fatty liver is present and there are no other causes of liver injury, including alcoholic or viral liver disease[1,2]. The accumulation of triglycerides in the liver is a relatively benign condition and is the result of a mechanism that protects the liver by converting incoming harmful fatty acids into relatively safe forms. However, in some fatty liver patients, the condition progresses to non-alcoholic steatohepatitis (NASH), which is characterized by persistent hepatitis, tissue damage, and liver fibrosis[2]. In particular, liver fibrosis correlates most strongly with prognosis and mortality in NASH patients because it can progress to cirrhosis and hepatocarcinoma[3]. The prevalence of NAFLD and NASH continues to increase and has reached 30% and 12%, respectively, in the United States[4]. Liver disease due to NASH is predicted to become a major cause of liver transplantation[5]. Accordingly, drug development for NAFLD/NASH has become a research priority. Clinical trials are underway for many candidate compounds. While a drug treatment for NAFLD/NASH will likely be available in the near future, no approved treatment presently exists. Factors hindering drug development include the complex and poorly understood mechanisms of NAFLD/NASH pathogenesis, a very heterogeneous liver disease that is unlikely to respond to a single-drug approach, and the lack of a gold standard animal model.

The etiology of the progression from simple fatty liver to NASH remains unclear. The “two-hit hypothesis” proposed that the first hit, hepatic steatosis, is followed by a second hit, stress, which causes inflammation and liver injury. The latter lead to the progression to NASH. This hypothesis does not adequately explain some of the molecular and metabolic changes that occur in NAFLD and is now considered outdated. The “multiple-hit hypothesis” proposes that NASH is induced by the addition of multiple factors in genetically predisposed patients[6,7]. These factors include insulin resistance, hormones, and gut microbiota. In recent years, metabolic (dysfunction)-associated fatty liver disease (MAFLD) has been proposed, considering its close association with metabolic abnormalities[8,9]. In fact, NAFLD is frequently complicated by various dysmetabolic diseases, such as obesity, type 2 diabetes, dyslipidemia, and chronic kidney disease[10–15].

An ideal animal model would mimic the pathophysiology of NASH in humans. It should have the typical features of NASH, such as obesity, liver fat deposition, inflammation, and ballooning. For drug development, it is also important to assess liver fibrosis, which is highly correlated with NASH prognosis. Animal models of NASH used in non-clinical settings can be classified into three categories: dietary burden, genetically modified, and drug-induced models[16]. Dietary burden models are frequently used because of their simplicity. However, their drawback is that long-term dietary challenges are required for the development of NASH pathophysiology.

In the context of NAFLD/NASH, we focused on the possibility of animal models of NASH caused by the hepatic accumulation of cholesterol as the cause of metabolic abnormalities. Liver is important

in cholesterol homeostasis. Similar to triglycerides, cholesterol esters are a relatively safe form of lipid storage. However, accumulation of free cholesterol in the liver is highly toxic to multiple intracellular processes and organelles[17]. Although there are many cholesterol-loaded NASH models, a model of very early onset of NASH pathology has recently been reported in mice fed a high-fat, high-cholesterol, and cholic acid-containing diet with hydroxypropyl-β-cyclodextrin (CDX) water[18,19]. In these reports, CDX was used to increase cholesterol absorption.

We evaluated the potential of cholesterol overload and its absorption enhancement in Sprague-Dawley (SD) rats as a new NAFLD/NASH model. We measured liver steatosis, inflammation, and fibrosis-related parameters in response to high-fat and cholesterol loads and determined the pathogenesis of NASH pathology in the rats. In addition, we investigated oxidative stress and endoplasmic reticulum (ER) stress in the liver.

Methods

Animals

Four-week-old female SD rats were purchased from CLEA Japan (Tokyo, Japan) and acclimatized for 2 weeks. Female rats were chosen because CDX toxicity occurs at lower doses in male rats than in females[20]. The animals were kept individually in cages in a room climate-controlled for temperature (23±3°C), humidity (55±15%), and lighting (12 h dark-light cycle). At 6 weeks of age, the animals were divided into three groups (n=6 per group) with equal mean values for body weight, blood aspartate aminotransferase (AST), alanine aminotransferase (ALT), and total cholesterol (TC) levels. During the experimental period, each group of animals was fed a normal diet (CRF-1, Oriental Yeast Co., Ltd., Tokyo, Japan) with normal water (control group); high-fat (60 kcal%), cholesterol (1.25%), and cholic acid (0.5%) diet (HFCC; D11061901, Research Diets, New Brunswick, New Jersey, USA) with normal water (HFCC group); or HFCC diet with 2% CDX water (HFCC+CDX group). The animals were dissected at 22 weeks of age and liver samples were collected. All animals were handled in strict compliance with the laboratory guidelines for animal experimentation set by the Ethics Committee for Animal Use at Central Pharmacological Research Institute, Japan Tobacco Inc. Body weights were measured at 6, 10, 14, 18, and 22 weeks of age. Daily calorie intake was calculated from the average daily food intake (g/day) at 6, 10, 14, 18, and 22 weeks of age and calorie per weight of the normal diet (CRF-1; 3.57 kcal/g) and HFCC diet (D11061901; 4.80 kcal/g).

Tissue sampling and immunostaining

All animals were exsanguinated and dissected under isoflurane anesthesia at 22 weeks of age. Liver samples were collected for lipid content measurement, gene expression analysis, and histopathological evaluation. Intestinal samples were collected for gene expression analysis. Samples other than those

used for pathological evaluation were stored at -80°C until use. Histopathological evaluation was performed as described previously[21,22]. Liver samples for pathological evaluation were fixed in 10% neutral-buffered formalin immediately after collection. The fixed tissues were paraffin-embedded and thinly sliced (3–5 μm). The prepared liver sections were stained with hematoxylin and eosin (H&E) or Sirius Red for pathological evaluation. The prepared Sirius Red stained slides were observed under a microscope and the multiple perivenular areas were photographed. The images were captured using analysis software (inForm, Akoya Biosciences, Marlborough, MA, USA), and the area fraction of the stained area was calculated.

Hepatic lipid contents

The liver was removed from each rat and approximately 100 mg of each section was collected in tubes. Zirconia beads and methanol (0.5 mL) were added to the tube and the samples were homogenized using a model MM300 mixer mill (Retsch GmbH, Haan, Germany) at 25 Hz for 10 min. One milliliter of chloroform was added to all homogenates, mixed well, and centrifuged (10,000 × *g*, 5 min, 4°C) to extract lipids. Then, 0.2 mL of the supernatant was dried with nitrogen gas for approximately 40 min. The residue was redissolved in 0.5 mL 2-propanol and used for subsequent lipid measurements. Levels of triglyceride (TG), TC, phospholipid (PL), and non-esterified fatty acid (NEFA) in the liver extract were measured using a model 3500 biochemistry automatic analyzer (Hitachi, Tokyo, Japan). Lipid hydroperoxide (LPO) content was determined using the LPO-CC kit (Kamiya Biomedical Company, Seattle, WA, USA) according to the manufacturer's protocol.

Biological parameters

Blood samples were collected from the tail vein of all rats at 6, 14, and 22 weeks of age for biochemical measurements of AST, ALT, glucose (GLU), TC, TG, and PL. These levels were measured using respective product kits (Roche Diagnostics, Tokyo, Japan) and an automatic analyzer (Hitachi).

RNA extraction and real-time quantitative PCR analysis

Total RNA was prepared from approximately 20 mg of liver or small intestine samples using the GenElute™ Mammalian Total RNA Miniprep Kit (MilliporeSigma, Burlington, MA, USA), according to the manufacturer's protocols. Extracted RNA was suspended in DNAse/RNAse-free water and its concentration was measured using a NanoDrop spectrophotometer (Thermo Fisher Scientific, Waltham, MA, USA).

Reverse transcription of 1 μg of total RNA to complementary DNA (cDNA) was performed using the High-Capacity cDNA Reverse Transcription Kit with an RNase Inhibitor (Applied Biosystems, Foster City, CA, USA) to synthesize cDNA. Reverse transcription reactions were performed using the

following temperature and time cycles: 25°C for 10 min, 37°C for 120 min, and 85°C for 5 min.

Gene expression was quantified by real-time PCR using QuantStudio 7 Flex (Thermo Fisher Scientific) and TaqMan Gene Expression Assays (Table 1). The reaction mixture for real-time PCR contained 10 ng of cDNA. The temperature and time cycles were 10 min at 95°C, followed by 40 cycles of 15 s at 95°C, and 60 s at 60°C.

Statistical analyses

All values are expressed as mean ± standard deviation. The multiple-group test was performed as follows. Initially, equal variances were assessed using the Bartlett's test. The Tukey–Kramer method was used to analyze the homoscedasticity data. Otherwise, the Steel-Dwass method was used as a nonparametric test for heteroscedastic data. Two-way repeated measure ANOVA followed by Tukey's multiple comparison test was performed for analyzing time course of each parameter between three groups. All statistical analyses were performed using GraphPad Prism® 9.0.1 (GraphPad Software, San Diego, CA, USA). For all tests, statistical significance was set at $P<0.05$.

Results

Weight change by HFCC or HFCC + CDX feeding

The HFCC or HFCC+CDX feeding period for female SD rats was set at 16 weeks. This period was selected because preliminary results from an 8-week feeding study suggested that a longer period was necessary. During the study period, there was significant gain in body weight of rats in the HFCC group compared to that of rats in the control group. In contrast, the HFCC+CDX group showed no weight gain compared with the control group throughout the study period (Fig. 1A). The daily caloric intake did not change in any of the groups throughout the study period (Fig. 1B). In addition, there was no evidence of overeating or significant obesity in this model.

Changes in blood biochemistry values by HFCC or HFCC+CDX feeding

Blood AST, ALT, TC, and PL were significantly elevated after 16 weeks of HFCC or HFCC+CDX feeding compared to control (Fig. 1C, D, F, H). Blood ALT tended to be higher in the HFCC+CDX group than in the HFCC group at 8 weeks (14 weeks of age) of feeding (Fig. 1D). At this point, excessive cholesterol intake and liver damage began to occur. On the other hand, blood GLU was slightly elevated only in the HFCC group (Fig. 1E). No significant changes were observed in the blood TG levels throughout the study period (Fig. 1G). Adequate cholesterol feeding and hepatic injury were observed throughout the study.

Effects of cholesterol loading on liver weight and hepatic lipids

Analysis of liver lipid content revealed fatty liver formation as a major component of NAFLD pathogenesis. At 16 weeks after the start of feeding (22 weeks of age), significant increases in hepatic TG, TC, NEFA, and LPO levels and liver weight per body weight were observed in the HFCC and HFCC+CDX groups compared to the control (Fig. 2A-C, E, F). Furthermore, hepatic PL content was significantly lower (Fig. 2D). Contrary to expectations, however, liver TC content did not increase in the HFCC+CDX group compared to that in the HFCC alone group (Fig. 2C). These results suggest that the HFCC diet induces hepatic lipid and cholesterol accumulation.

Liver histopathologic evaluation

Histopathological analysis of the liver is the most important evaluation method used to definitively diagnose NASH. We evaluated H&E-stained specimens for hepatosteatosis, hepatocyte hypertrophy, and inflammatory cell infiltration in the liver (Fig. 3A, Table 2). Animals in the control group showed no pathological changes in any of the parameters. In contrast, all animals in the HFCC and HFCC+CDX groups showed fatty liver and inflammatory cell infiltration. Large lipid droplets in the liver, a hallmark of NASH pathology, tended to be observed more in animals in the HFCC+CDX group than in those in the HFCC group.

The degree of liver fibrosis is an important indicator that strongly correlates with the prognosis of patients with NASH. Sirius Red-stained specimens and analysis of the positive area fraction were used to evaluate the progression of liver fibrosis in all animals (Fig. 3A, B). Sirius Red staining of the tissue surrounding the vessel wall was stronger in animals in the HFCC group compared to the control group, but no significant change in the fibrosis area fraction was observed. In contrast, in the HFCC+CDX group, Sirius Red staining was observed between the liver parenchymal tissues and the fibrosis area ratio increased significantly. These results suggest that HFCC with CDX intake might have caused more severe NASH pathogenesis than the HFCC diet alone.

Gene expression analysis in liver and intestinal tract

Fig. 4 shows the expression analysis results of NASH pathogenesis-related genes in the liver. The mRNA expression levels of lipid synthesis-related genes (*Srebp1*, *Scd1*, and *Pemt*), inflammation-related genes (*Tnf*, *Ccl2*, and *Il6*), and fibrosis-related genes (*Col1a1*, *Acta2*, and *Tgfb*) were compared. Consistent with the results of changes in liver TG content (Fig. 2B), expression levels of the lipogenesis gene *Scd1* and its transcription factor *Srebp1* were significantly elevated in the HFCC and HFCC+CDX groups compared to the control (Fig. 4A, B). In contrast, the expression of *Pemt*, which plays an important role in phospholipid synthesis, decreased in the loaded groups (Fig. 4C), suggesting a possible influence on the decreased PL content in the liver. Compared to the control group, upregulation of inflammation- and fibrosis-related gene expression in the liver was observed in both the HFCC and HFCC+CDX groups (Fig. 4D-I). In addition, the HFCC+CDX group tended to have a

greater upregulation of inflammation-related genes than the HFCC group, although without a significant difference (Fig. 4D-F).

We then evaluated changes in the expression of genes related to cholesterol metabolism and ER stress in the liver and genes contributing to lipid absorption in the intestinal tract. There was a trend toward a decrease or significant decrease in hepatic *Srebp2* and gut *Npc1l1* mRNA expression in the HFCC and HFCC+CDX groups (Fig. 4J, O). The significant downregulation of hepatic *Fxr* in these groups (Fig. 4K) may contribute to the induction of NASH pathogenesis. Cholesterol accumulation in the liver causes liver damage, mainly through ER stress. The expression of the ER stress-related gene *Atf4* in the liver was elevated only in the HFCC+CDX group (Fig. 4M).

Discussion

The lack of animal disease models hinders the elucidation of pathomechanisms and complicates drug development. In response to the lack of animal models of NASH, we validated the use of a cholesterol overload and absorption enhancement to create a new rat model of NASH that features more severe disease formation. SD rats were fed a high-fat, high-cholesterol, and cholic acid-containing diet with CDX. In a previous study, it was reported that HFCC+CDX feeding in mice can induce NASH pathology with fatty liver, inflammation, and mild fibrosis within 3 weeks[18,19]. Accordingly, we subjected SD rats to this dietary load to determine whether the pathophysiology could be made more severe compared to that in a simple cholesterol-induced NASH model.

The diet used in this study contained cholic acid. This bile acid is involved in the reduction of hepatic NEFA, TG, and very-low-density lipoprotein synthesis via farnesoid X receptor (FXR) signaling. In addition, mice fed a high-fat diet containing cholic acid reportedly displayed inhibited body weight gain due to increased energy expenditure[23]. Thus, while cholic acid might improve NASH pathology, it can also increase cholesterol absorption in the intestinal tract and induce multiple collagen-related genes in the liver[24,25]. In rats, high-fat, cholesterol, and cholate diets have been reported to cause hyperlipidemia, hyperglycemia, and liver damage[26]. Cholic acid is often used in the diet to create NASH models. CDX is a cyclodextrin derivative with practical pharmaceutical, cosmetic, and industrial applications. CDX has hydrophobic cavities inside its ring structure, enabling the uptake organic compounds and other substances to increase their solubility. It has been suggested that the inclusion complex formation of CDX with cholesterol makes the latter more water-soluble than cholesterol alone[27], thereby promoting cholesterol absorption in the gut. On the other hand, cyclodextrins are known to form inclusion complexes with various bile acids in aqueous solution. It is possible that the hydroxyl-β-cyclodextrin used in this study, like other cyclodextrins, forms inclusion complexes with cholic acid, resulting in increased absorption of cholic acid. In other words, the HFCC+CDX group showed a greater effect of cholic acid on energy expenditure and may have

reduced weight gain. Because of these characteristics of CDX, it is necessary to pay attention to changes in its absorbency when using this model to evaluate drugs. In other words, the dosage of the compound should be carefully controlled, and its pharmacological effects should be evaluated.

In this study, NASH-like pathogenesis of fatty liver and hepatitis was observed in all animals treated with HFCC or HFCC+CDX for 16 weeks. Elevated liver NEFA and LPO levels may contribute to liver injury from lipotoxicity and oxidative stress, respectively. Decreased hepatic PL is one of the features observed in NASH. In addition, Sirius Red staining of the liver tissue in the HFCC+CDX group revealed a significant increase in the fibrotic area fraction. The trend toward higher expression levels of liver inflammation-related gene markers in the HFCC+CDX group than in the HFCC group, together with significantly higher expression of ER stress-related genes, suggests that NASH pathology was more potently induced by the presence of CDX. However, there was no significant difference in the liver TC content between the HFCC and HFCC+CDX groups. The cause of this discrepancy remains unclear. CDX-induced toxicity induced by oral intake in female rats has been previously studied. Oral CDX intake of 5000 mg/kg/day for 12 months resulted in increased body weight, leukocytosis, thrombocytopenia, and lung abnormalities, with no evidence of toxicity in the liver[20]. Therefore, it is unlikely that CDX-induced toxicity was the cause of the more severe NASH pathology that we observed in the HFCC+CDX group. Several data points led us to consider the possibility that there is a difference in the speed of pathogenesis. Eight weeks after the start of feeding (14 weeks of age), blood ALT levels were higher in the HFCC+CDX group. Preliminary studies also showed increased expression of liver inflammation- and fibrosis-related markers in the HFCC+CDX group at the same time point (8 weeks after the start of feeding; data not shown). This suggests that accelerated cholesterol absorption in the CDX-loaded group might have contributed to an earlier plateau in hepatic cholesterol accumulation, leading to more severe NASH pathogenesis. Evaluations of liver TC content and other NASH-related parameters from early autopsies are needed to confirm this suggestion.

Despite increased expression of liver fibrosis-related genes in the HFCC group, histopathological analysis revealed no progression of liver fibrosis. This result seemingly contradicts the results of the histopathological evaluation of liver fibrosis. It is possible that HFCC alone induced liver fibrosis but did not reach a definite pathological stage.

Hydroxymethylglutaryl-CoA (HMG-CoA) reductase and low-density lipoprotein (LDL) receptor, which play important roles in cholesterol homeostasis in the liver, are regulated by sterol regulatory element-binding protein 2. An important pathway for cholesterol metabolism in the liver is its conversion to bile acids and their excretion, which is controlled by the FXR and other nuclear receptors. In the present study, the expression of these two key genes was significantly downregulated in the HFCC and HFCC+CDX groups. This may be a feedback response to the accumulation of cholesterol in the liver to inhibit its synthesis and uptake. The gene expression of *Fxr* is important for inhibiting

cytotoxic bile acid synthesis and promoting efflux[28,29]. It is very likely that reduced *Fxr* activity contributes to cholesterol accumulation in the liver. In addition, FXR in hepatic stellate cells reportedly induces cell quiescence and apoptosis-promoting phenotypes that promote resolution of hepatic fibrosis[30]. The importance of FXR as a crucial nuclear receptor in NASH pathogenesis is evidenced by the many drugs targeting FXR that are being explored as NASH treatments. Reduced *Fxr* expression is an important feature of our novel animal model.

Similar to our study, several previous reports described NASH models in which rats were fed high-fat, high-cholesterol, and cholic acid diets[31,32]. Ichimura *et al.* described a diet composition similar to ours. The authors observed significantly decreased expression levels of *Srebp2* and *Fxr* as cholesterol- and bile acid-related genes in the liver, which is consistent with our results, while their model showed more advanced NASH pathology, including liver fibrosis[32]. The fact that the HFCC feeding period of their animals was 2 weeks longer than ours might not be a sufficient explanation for this difference. We focused on differences in the pathogenesis of NASH between the sexes of rats. In our model, female SD rats were used to eliminate the toxic effects of orally ingesting CDX. It is well known that the incidence of NASH is higher in males than in females in humans[33]. This is considered to be due to the antimetabolic syndrome and hepatoprotective effects of female hormones[34]. In addition to the influence of sex hormones, the female-specific phase of the ovarian cycle may also influence the degree of NASH pathogenesis. We cannot rule out the possibility that the limitation of using female rats to establish the NASH model might have resulted in milder NASH pathology compared to male rats subjected to a similar high-cholesterol load.

A typical rat model of NASH is the choline-deficient L-amino denatured (CDAA) diet model [35] which is superior to the HFCC+CDX model in that the progression of NASH is rapid, but the mechanism is different. The CDAA diet causes increased lipid synthesis in the rat liver and decreased TG secretion from the liver, leading to marked hepatic steatosis in a short period of time. In other words, the type of lipid accumulation in the liver may be different from the HFCC+CDX model where cholesterol accumulation is predominant. In human NASH, a correlation between cholesterol and pathophysiology has been consistently reported [17] and the HFCC+CDX model may be a more useful model and potentially a better model for studying NASH pathophysiology in relation to cholesterol.

It is possible that differences in diet and cholesterol metabolism between mice and rats may have contributed to the difference in the time required for NASH pathogenesis with the same HFCC+CDX diet. Because rats lack a gallbladder, they are unable to store bile acids, the major metabolite of cholesterol, and cholesterol clearance may be faster in rats than in mice. There are also significant differences between humans and mice/rats. Specifically, the type of major lipoproteins in the blood and the presence or absence of cholesteryl ester transfer protein. The details of how these differences may contribute to the pathogenesis of NASH are not clear. However, the consistently reported correlation between cholesterol and the development of NASH in humans and the findings in

HFCC+CDX mice in the previous study and in HFCC+CDX rats in the present study certainly suggest that cholesterol is an important factor in NASH. Although the feeding of female SD rats with HFCC+CDX has some limitations, such as the lack of body weight gain, it may provide useful information for future animal model studies, showing that the enhancement of cholesterol absorption in rats may promote NASH-like pathology.

In conclusion, we successfully induced NASH-like pathogenesis in female SD rats by feeding HFCC diet. HFCC+CDX feeding induced abnormal hepatic cholesterol homeostasis, a tendency to upregulate inflammation-related marker genes, and induction of ER stress. As a result, liver fibrosis was exacerbated. These results suggest the possibility of a new NASH model that focuses on cholesterol overload and accelerated absorption.

Conflict of Interest

Yasuka Saigo, Tomohiko Sasase, Yuichi Shinozaki, Tatsuya Maekawa, and Ryuhei Sano are employees of Japan Tobacco Inc. Marika Tohma, Kinuko Uno, Katsuhiro Miyajima, and Takeshi Ohta have no conflict of interest.

References

1. Estes C, Razavi H, Loomba R, Younossi Z, Sanyal AJ. Modeling the epidemic of nonalcoholic fatty liver disease demonstrates an exponential increase in burden of disease: Estes et al. Hepatology 2018;67(1):123–33.

2. Friedman SL, Neuschwander-Tetri BA, Rinella M, Sanyal AJ. Mechanisms of NAFLD development and therapeutic strategies. Nat Med 2018;24(7):908–22.

3. Younossi ZM, Koenig AB, Abdelatif D, Fazel Y, Henry L, Wymer M. Global epidemiology of nonalcoholic fatty liver disease-Meta-analytic assessment of prevalence, incidence, and outcomes: 2016. Hepatology 2016;64(1):73–84.

4. Charlton MR, Burns JM, Pedersen RA, Watt KD, Heimbach JK, Dierkhising RA. Frequency and Outcomes of Liver Transplantation for Nonalcoholic Steatohepatitis in the United States. Gastroenterology 2011;141(4):1249–53.

5. Sheka AC, Adeyi O, Thompson J, Hameed B, Crawford PA, Ikramuddin S. Nonalcoholic Steatohepatitis: A Review. JAMA 2020;323(12):1175.

6. Fang Y-L, Chen H, Wang C-L, Liang L. Pathogenesis of non-alcoholic fatty liver disease in children and adolescence: From “two hit theory” to “multiple hit model.” World J Gastroenterol 2018;24(27):2974–83.

7. Buzzetti E, Pinzani M, Tsochatzis EA. The multiple-hit pathogenesis of non-alcoholic fatty liver disease (NAFLD). Metabolism 2016;65(8):1038–48.

8. Eslam M, Sanyal AJ, George J, Sanyal A, Neuschwander-Tetri B, Tiribelli C, Kleiner DE, Brunt E, Bugianesi E, Yki-Järvinen H, Grønbæk H, Cortez-Pinto H, George J, Fan J, Valenti L, Abdelmalek M, Romero-Gomez M, Rinella M, Arrese M, Eslam M, Bedossa P, Newsome PN, Anstee QM, Jalan R, Bataller R, Loomba R, Sookoian S, Sarin SK, Harrison S, Kawaguchi T, Wong VW-S, Ratziu V, Yilmaz Y, Younossi Z. MAFLD: A Consensus-Driven Proposed Nomenclature for Metabolic Associated Fatty Liver Disease. Gastroenterology 2020;158(7):1999-2014.e1.

9. Lonardo A, Leoni S, Alswat KA, Fouad Y. History of Nonalcoholic Fatty Liver Disease. Int J Mol Sci 2020;21(16):E5888.

10. Chaney A. Obesity and Nonalcoholic Fatty Liver Disease. Nurs Clin North Am 2021;56(4):543–52.

11. Luo Y, Lin H. Inflammation initiates a vicious cycle between obesity and nonalcoholic fatty liver disease. Immun Inflamm Dis 2021;9(1):59–73.

12. Younossi ZM, Golabi P, de Avila L, Paik JM, Srishord M, Fukui N, Qiu Y, Burns L, Afendy A, Nader F. The global epidemiology of NAFLD and NASH in patients with type 2 diabetes: A systematic review and meta-analysis. J Hepatol 2019;71(4):793–801.

13. Xu Y, Yang X, Bian H, Xia M. Metabolic dysfunction associated fatty liver disease and coronavirus disease 2019: clinical relationship and current management. Lipids Health Dis 2021;20(1):126.

14. Lee WM, Bae JH, Chang Y, Lee SH, Moon JE, Jeong SW, Jang JY, Kim SG, Kim HS, Yoo J-J, Kim YS. Effect of Nutrition Education in NAFLD Patients Undergoing Simultaneous Hyperlipidemia Pharmacotherapy: A Randomized Controlled Trial. Nutrients 2021;13(12):4453.

15. Byrne CD, Targher G. NAFLD as a driver of chronic kidney disease. J Hepatol 2020;72(4):785–801.

16. Febbraio MA, Reibe S, Shalapour S, Ooi GJ, Watt MJ, Karin M. Preclinical Models for Studying NASH-Driven HCC: How Useful Are They? Cell Metab 2019;29(1):18–26.

17. Horn CL, Morales AL, Savard C, Farrell GC, Ioannou GN. Role of Cholesterol-Associated Steatohepatitis in the Development of NASH. Hepatol Commun 2022;6(1):12-35.

18. Duparc T, Briand F, Trenteseaux C, Merian J, Combes G, Najib S, Sulpice T, Martinez LO. Liraglutide improves hepatic steatosis and metabolic dysfunctions in a 3-week dietary mouse model of nonalcoholic steatohepatitis. Am J Physiol Gastrointest Liver Physiol 2019;317(4):G508–17.

19. Briand F, Heymes C, Bonada L, Angles T, Charpentier J, Branchereau M, Brousseau E, Quinsat M, Fazilleau N, Burcelin R, Sulpice T. A 3-week nonalcoholic steatohepatitis mouse model shows elafibranor benefits on hepatic inflammation and cell death. Clin Transl Sci 2020;13(3):529–38.

20. Gould S, Scott RC. 2-Hydroxypropyl-β-cyclodextrin (HP-β-CD): A toxicology review. Food Chem Toxicol 2005;43(10):1451–9.

21. Toriniwa Y, Muramatsu M, Ishii Y, Riya E, Miyajima K, Ohshida S, Kitatani K, Takekoshi S, Matsui T, Kume S, Yamada T, Ohta T. Pathophysiological characteristics of non-alcoholic steatohepatitis-like changes in cholesterol-loaded type 2 diabetic rats. Physiol Res 2018;67(4):601–12.

22. Saito T, Muramatsu M, Ishii Y, Saigo Y, Konuma T, Toriniwa Y, Miyajima K, Ohta T. Pathophysiological analysis of the progression of hepatic lesions in STAM mice. Physiol Res 2017;66(5):791–9.

23. Watanabe M, Houten SM, Mataki C, Christoffolete MA, Kim BW, Sato H, Messaddeq N, Harney JW, Ezaki O, Kodama T, Schoonjans K, Bianco AC, Auwerx J. Bile acids induce energy expenditure by promoting intracellular thyroid hormone activation. Nature 2006;439(7075):484–9.

24. Murphy C, Parini P, Wang J, Björkhem I, Eggertsen G, Gåfvels M. Cholic acid as key regulator of cholesterol synthesis, intestinal absorption and hepatic storage in mice. Biochim Biophys Acta 2005;1735(3):167–75.

25. Vergnes L, Phan J, Strauss M, Tafuri S, Reue K. Cholesterol and cholate components of an atherogenic diet induce distinct stages of hepatic inflammatory gene expression. J Biol Chem 2003;278(44):42774–84.

26. Jamshed H, Arslan J, Gilani A-H. Cholesterol-cholate-butterfat diet offers multi-organ dysfunction in rats. Lipids Health Dis 2014;13:194.

27. Williams III RO, Mahaguna V, Sriwongjanya M. Characterization of an inclusion complex of cholesterol and hydroxypropyl-β-cyclodextrin. Eur J Pharm Biopharm 1998;46(3):355–60.

28. Li T, Matozel M, Boehme S, Kong B, Nilsson L-M, Guo G, Ellis E, Chiang JYL. Overexpression of cholesterol 7α-hydroxylase promotes hepatic bile acid synthesis and secretion and maintains cholesterol homeostasis. Hepatol Baltim Md 2011;53(3):996–1006.

29. Lambert G, Amar MJA, Guo G, Brewer HB, Gonzalez FJ, Sinal CJ. The farnesoid X-receptor is an essential regulator of cholesterol homeostasis. J Biol Chem 2003;278(4):2563–70.

30. Fiorucci S, Rizzo G, Antonelli E, Renga B, Mencarelli A, Riccardi L, Orlandi S, Pruzanski M, Morelli A, Pellicciari R. A farnesoid x receptor-small heterodimer partner regulatory cascade modulates tissue metalloproteinase inhibitor-1 and matrix metalloprotease expression in hepatic stellate cells and promotes resolution of liver fibrosis. J Pharmacol Exp Ther 2005;314(2):584–95.

31. Horai Y, Utsumi H, Ono Y, Kishimoto T, Ono Y, Fukunari A. Pathological characterization and morphometric analysis of hepatic lesions in SHRSP5/Dmcr, an experimental non-alcoholic steatohepatitis model, induced by high-fat and high-cholesterol diet. Int J Exp Pathol 2016;97(1):75–85.

32. Ichimura M, Masuzumi M, Kawase M, Sakaki M, Tamaru S, Nagata Y, Tanaka K, Suruga K, Tsuneyama K, Matsuda S, Omagari K. A diet-induced Sprague–Dawley rat model of nonalcoholic steatohepatitis-related cirrhosis. J Nutr Biochem 2017;40:62–9.

33. Lonardo A, Nascimbeni F, Ballestri S, Fairweather D, Win S, Than TA, Abdelmalek MF, Suzuki A. Sex Differences in Nonalcoholic Fatty Liver Disease: State of the Art and Identification of Research Gaps. Hepatology 2019;70(4):1457–69.

34. Farruggio S, Cocomazzi G, Marotta P, Romito R, Surico D, Calamita G, Bellan M, Pirisi M, Grossini E. Genistein and 17β-Estradiol Protect Hepatocytes from Fatty Degeneration by Mechanisms Involving Mitochondria, Inflammasome and Kinases Activation | Cell Physiol Biochem. Cell Physiol Biochem 2020;54(3):401–16.

35. Nakae D, Yoshiji H, Mizumoto Y, Horiguchi K, Shiraiwa K, Tamura K, Denda A, Konishi Y. High incidence of hepatocellular carcinomas induced by a choline deficient L-amino acid defined diet in rats. Cancer Res 1992;52(18):5042–5.

Table 1 TaqMan Gene Expression Assays used for real-time PCR

Gene classification	Gene name	TaqMan ID
Liver lipid-related genes	*Scd1*	Rn06152614_s1
	Srebp1	Rn01495769_m1
	Srebp2	Rn01502638_m1
	Pemt	Rn00564517_m1
	Fxr	Rn00572658_m1
Liver fibrosis-related genes	*Col1a1*	Rn01463848_m1
	Acta2	Rn01759928_g1
	Tgfb	Rn99999016_m1
Liver inflammation-related genes	*Tnf*	Rn99999017_m1
	Ccl2	Rn00580555_m1
	Il6	Rn01410330_m1
Liver ER stress-related genes	*Chop*	Rn00492098_g1
	Atf4	Rn00824644_g1
Gut absorption-related genes	*Cd36*	Rn00580728_m1
	Npc1l1	Rn01443503_m1
Endogenous control gene	*Gapdh*	Rn99999916_s1

Table 2 Histopathological findings in liver

	Control						HFCC						HFCC+CDX					
	1	2	3	4	5	6	1	2	3	4	5	6	1	2	3	4	5	6
Hepatosteatosis (Vacuolation/Fatty change)	–	–	–	–	–	–	±	±	+	+	±	±	±	+	+	±	+	2+
Hypertrophy of hepatocytes	–	–	–	–	–	–	+	+	+	+	±	±	±	+	±	+	+	+
Infiltration, inflammatory cells	–	–	–	–	–	–	±	+	±	±	±	±	+	+	±	±	±	±

–, negative; ±, very slight; +, slight; 2+, moderate; 3+, severe

The results are the summary of pathological evaluation by H&E staining (hepatosteatosis and hypertrophy of hepatocytes) (n=6)

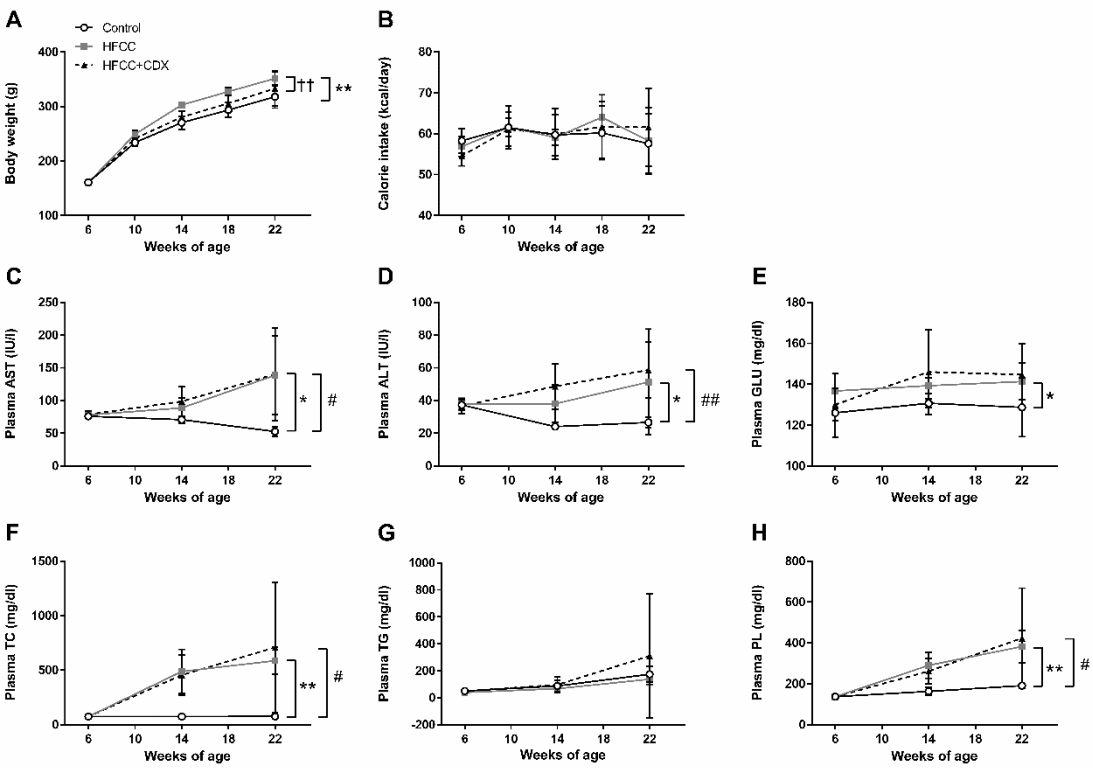

Fig. 1 Body weight, daily caloric intake, and blood biochemical values

Average body weight and caloric intake at 6, 10, 14, 18, and 22 weeks of age, and blood biochemical values at 6, 14, and 22 weeks of age. (**A**) Body weight, (**B**) Daily caloric intake, (**C**) Plasma aspartate transaminase (AST), (**D**) Plasma alanine transaminase (ALT), (**E**) Plasma glucose (GLU), (**F**) Plasma total cholesterol (TC), (**G**) Plasma triglyceride (TG), (**H**) Plasma phospholipid (PL). Data represent the mean ± standard deviation (n=6). *P<0.05, **P<0.01 control vs. HFCC, #P<0.05, ##P<0.01 control vs. HFCC+CDX, ††P<0.01 HFCC vs. HFCC+CDX (two-way repeated measure ANOVA followed by Tukey's multiple comparison test). HFCC: high-fat, high-cholesterol, and cholic acid diet; CDX: hydroxypropyl-β-cyclodextrin

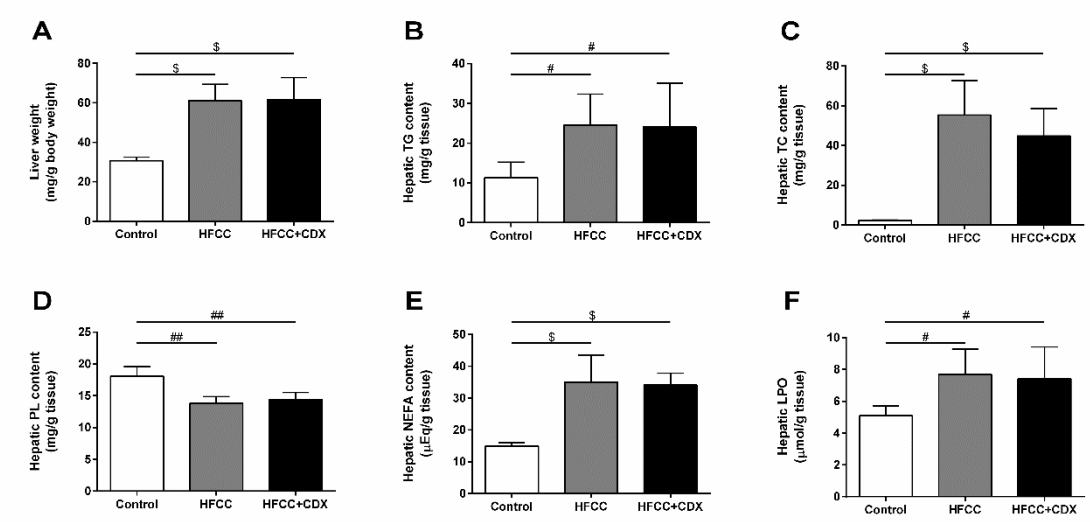

Fig. 2 Liver weight and liver lipid content at 22 weeks of age

(**A**) Liver weight (mg) per g body weight, (**B**) Liver triglyceride (TG), (**C**) Liver total cholesterol (TC), (**D**) Liver phospholipid (PL), (**E**) Liver non-esterified fatty acid (NEFA), (**F**) Liver lipid hydroperoxide (LPO). Data represent the mean ± standard deviation (n=6). #P<0.05, ##P<0.01 (Tukey-Kramer method, \$$P$<0.05, \$\$$P$<0.01 (Steel-Dwass method).

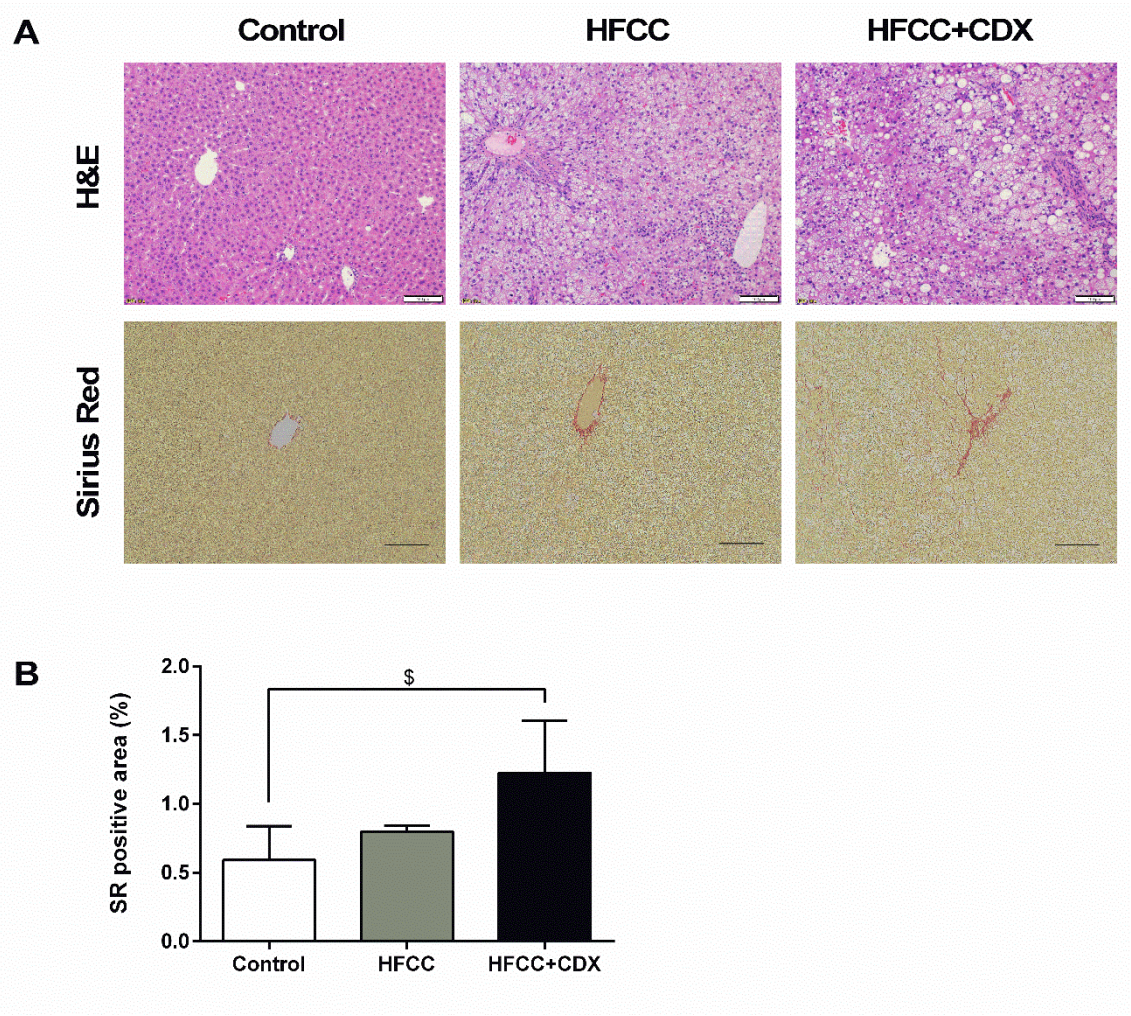

Fig. 3 Histopathology immunostaining of liver at 22 weeks of age

(**A**) Upper panel: H&E staining of liver sections (Scale bars: 100 μm); lower panel: Sirius Red staining of liver sections (Scale bars: 100 μm). (**B**) Sirius Red positive area fraction (%). Data represent the mean ± standard deviation (n=6). $$P<0.05$ (Steel-Dwass method).

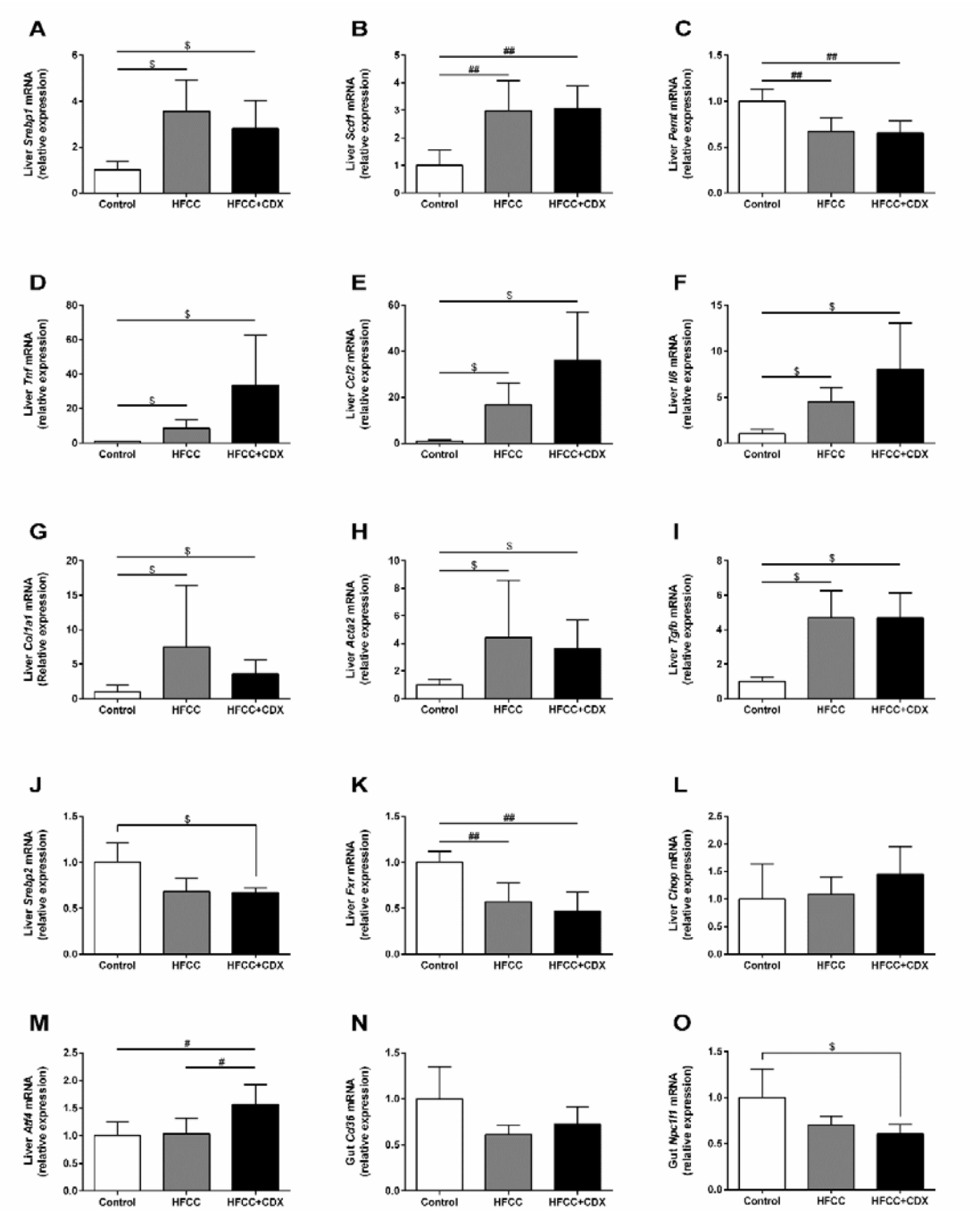

Fig. 4 Expression of genes related to lipid, inflammation, fibrosis, and ER stress in the liver and lipid absorption in the intestinal tract at 22 weeks of age

(**A**) Hepatic *Srebp1*, (**B**) hepatic *Scd1*, (**C**) hepatic *Pemt*, (**D**) hepatic *Tnf*, (**E**) hepatic *Ccl2*, (**F**) hepatic *Il6*, (**G**) hepatic *Col1a1*, (**H**) hepatic *Acta2*, (**I**) hepatic *Tgfb*, (**J**) hepatic *Srebp2*, (**K**) hepatic *Fxr*, (**L**) hepatic *Chop*, (**M**) hepatic *Atf4*, (**N**) gut *Cd36*, and (**O**) gut *Npc1l1*

Data represent the mean ± standard deviation (n=6). #P<0.05, ##P<0.01 (Tukey-Kramer method), \$$P$<0.05 (Steel-Dwass method).